HHS Public Access

Author manuscript

Sci Transl Med. Author manuscript; available in PMC 2015 March 19.

Published in final edited form as:

Sci Transl Med. 2014 February 12; 6(223): 223ra21. doi:10.1126/scitranslmed.3007244.

Local Hydrogel Release of Recombinant TIMP-3 Attenuates Adverse Left Ventricular Remodeling After Experimental Myocardial Infarction

Shaina R. Eckhouse[1], **Brendan P. Purcell**[2], **Jeremy R. McGarvey**[3], **David Lobb**[4], **Christina B. Logdon**[4], **Heather Doviak**[4], **Jason W. O'Neill**[5], **James A. Shuman**[4], **Craig P. Novack**[4], **Kia N. Zellars**[4], **Sara Pettaway**[4], **Roy A. Black**[5], **Aarif Khakoo**[5], **TaeWeon Lee**[5], **Rupak Mukherjee**[1], **Joseph H. Gorman**[3], **Robert C. Gorman**[3], **Jason A. Burdick**[2], and **Francis G. Spinale**[4,*]

[1]Cardiothoracic Surgery, Medical University of South Carolina, Charleston, SC 29425, USA

[2]Department of Bioengineering, University of Pennsylvania, Philadelphia, PA 19104, USA

[3]Gorman Cardiovascular Research Group, Department of Surgery, University of Pennsylvania, Philadelphia, PA 19104, USA

[4]Cardiovascular Translational Research Center, University of South Carolina School of Medicine and William Jennings Bryan Dorn Veteran Affairs Medical Center, Columbia, SC 29208, USA

[5]Amgen Incorporated, Seattle, WA 91320, USA

Abstract

An imbalance between matrix metalloproteinases (MMPs) and tissue inhibitors of MMPs (TIMPs) contributes to the left ventricle (LV) remodeling that occurs after myocardial infarction (MI). However, translation of these observations into a clinically relevant, therapeutic strategy remains to be established. The present study investigated targeted TIMP augmentation through regional injection of a degradable hyaluronic acid hydrogel containing recombinant TIMP-3 (rTIMP-3) in a large animal model. MI was induced in pigs by coronary ligation. Animals were then randomized

*Corresponding author. cvctrc@uscmed.sc.edu.

SUPPLEMENTARY MATERIALS

www.sciencetranslationalmedicine.org/cgi/content/full/6/223/223ra21/DC1

Fig. S1. Denatured rTIMP-3 has no effect on post-MI remodeling and MMP activity.

Table S1. ECM remodeling and cytokine expression after MI.

Table S2. Porcine-specific PCR arrays used in post-MI studies.

Author contributions: S.R.E., B.P.P., J.R.M., and D.L. carried out the experimentation involved in the testing and deployment of the hydrogels and rTIMP-3. C.B.L., H.D., J.W.O., J.A.S., C.P.N., K.N.Z., and S.P. were responsible for the technical aspects of the study, including echocardiography, animal management, TIMP-3 preparation, biological sample collection and analysis, immunoassays, PCR profiling and matrix measurements, and histological analysis, respectively. R.A.B., A.K., and T.L. designed, tested, and supervised the construction of the rTIMP-3 (His-tagged TIMP-3), analyzed the data, and interpreted the results. R.M. and J.H.G. were responsible for design, analysis, interpretation, data management, and final editing. R.C.G., J.A.B., and F.G.S. designed the study, executed and oversaw each component of the project, reviewed and analyzed the data and results, prepared the manuscript and figures, and performed final editing. R.M. and F.G.S. performed and supervised the final statistical analysis.

Competing interests: J.W.O., R.A.B., A.K., and T.L. are employees of Amgen Inc., which manufactures drugs for a wide range of diseases, including cardiovascular disease. The other authors declare that they have no competing interests.

Data and materials availability: The rTIMP-3 was furnished as a materials transfer agreement from Amgen to F.G.S.

to receive targeted hydrogel/rTIMP-3, hydrogel alone, or saline injection and followed for 14 days. Instrumented pigs with no MI induction served as referent controls. Multimodal imaging (fluoroscopy/ echocardiography/magnetic resonance imaging) revealed that LV ejection fraction was improved, LV dilation was reduced, and MI expansion was attenuated in the animals treated with rTIMP-3 compared to all other controls. A marked reduction in proinflammatory cytokines and increased smooth muscle actin content indicative of myofibroblast proliferation occurred in the MI region with hydrogel/rTIMP-3 injections. These results provide the first proof of concept that regional sustained delivery of an MMP inhibitor can effectively interrupt adverse post-MI remodeling.

INTRODUCTION

A structural milestone in the progression of heart failure after a myocardial infarction (MI) is left ventricular (LV) remodeling, defined as changes in LV geometry and structure. Although LV remodeling after MI is a multifactorial process, one ubiquitous event is that of infarct expansion. Specifically, infarct expansion is the regional process by which continuous turnover of the extracellular matrix (ECM) results in the LV wall thinning and the loss of structural support (1). One biological system that is active in the post-MI context is a family of ECM proteases, the matrix metalloproteinases (MMPs) (1–4). The induction and release of MMPs have been demonstrated in patients after MI and were associated with adverse LV remodeling and the development of heart failure, which was likely promulgated by infarct expansion (4). The cause-effect relationship between MMP induction and adverse LV remodeling has been established through systemic pharmacological MMP inhibition as well as transgenic constructs (1, 2). However, translation of systemic pharmacological MMP inhibition to clinical application has encountered problematic issues, including concerns surrounding dosing and potential side effects (1, 5).

Under ambient physiologic states, endogenous MMP inhibition is achieved through the synthesis and release of the tissue inhibitors of MMPs (TIMPs) (1, 6). In contradistinction to the induction of MMPs in the early post-MI period, a concomitant increase in relative TIMP levels may not occur, causing an imbalance between endogenous proteolytic activity and inhibition (4, 7). The biological effects of the four known TIMPs are not uniform, and their function is unique (1, 6, 8). Of particular relevance, transgenic deletion of TIMP-3 in mice has been shown to cause adverse remodeling and acceleration to heart failure (9). Unique biological features of TIMP-3 include a high affinity to bind to the ECM through interactions with glycosaminoglycans (10), an influence on cytokine processing (9), and the ability to alter fibroblast phenotype in vitro (8). Thus, localized augmentation of TIMP-3 in the context of post-MI remodeling constitutes a novel and translationally relevant therapeutic approach. Accordingly, the central hypothesis of this study was that regional delivery of exogenous TIMP-3 within the MI region reduces infarct expansion and alters the course of post-MI remodeling.

Hydrogels represent an attractive means for delivery of TIMP-3 to specific regions of the myocardium, and hydrogels have been used previously to localize and sustain the presentation of macromolecules in experimental models of MI (11). Past studies have also

demonstrated that composite materials such as those containing hydroxyapatite or fibrin-alginate can be safely injected into the myocardium of both large animals and humans (12, 13). Moreover, injectable hydrogels based on hyaluronic acid (HA), a glycosaminoglycan found abundantly in the ECM, have been deployed in large animal models of MI (11).

Thus, the goal of this study was to exploit the functionality of hydrogels to develop and implement a unique approach for local delivery of a recombinant TIMP-3 (rTIMP-3). Using a porcine model of MI, which demonstrates similar coronary anatomy, ventricular geometry, and response to ischemia to that of humans (14), we performed targeted injections of an HA hydrogel formulation, which achieved sustained release of rTIMP-3 into the MI region. Using this localized approach for rTIMP-3 delivery and relevant post-MI animal model, we observed a significant reduction in all of the major indices of adverse post-MI remodeling.

RESULTS

rTIMP-3 delivery from injectable hydrogels in vivo

The synthesized human rTIMP-3 demonstrated concentration-dependent inhibition of MMP activity in vitro (Fig. 1A). The HA gel was first formulated with reactive groups and a covalent gel formed by redox initiation (Fig. 1B). The rTIMP-3 (0.2 μg/μl) was then encapsulated into the HA gel (Fig. 1C). As shown in Fig. 1D, rTIMP-3 was successfully encapsulated in the gels and released at a nearly uniform rate during 14-day period when incubated in phosphate-buffered saline (PBS) supplemented with bovine serum albumin at 37°C. A substantial amount of rTIMP-3 remained in the gels after the 14-day study, suggesting that the release of rTIMP-3 from the gels can be sustained for more than 14 days, which was the prespecified interval of interest for the in vivo post-MI efficacy studies. This time interval encompasses when a rapid acceleration of the post-MI remodeling process occurs and is associated with MMP release in patients (4).

For the in vivo validation studies, the HA gels containing rTIMP-3 were injected into a targeted myocardial region [nine injection sites, 100 μl per injection containing rTIMP-3 (0.2 μg/μl)] (Fig. 1E). After 7 days, rTIMP-3 was detected at each of the injection sites, but no signal was obtained in nontargeted areas (Fig. 1F). Histological examination 24 and 48 hours after injection revealed that the HA gels remained localized to the targeted injection sites (Fig. 1G). Moreover, at 7 days after injection, a positive rTIMP-3 signal by immunoblotting was detected, with no positive signal for rTIMP-3 identified in liver, kidney, lung, or blood samples (Fig. 1H).

Because the LV region targeted for injection was precisely defined (2×2 cm^2; Fig. 1E), and assuming a maximum injection depth of 1 cm [as quantified by echocardiography and cardiac magnetic resonance imaging (cMRI)], the volume of the targeted injection region was calculated as 4 cm^3. On the basis of the release kinetics determined in initial studies (Fig. 1D; ~200 ng of rTIMP-3 released per milliliter of hydrogel per day) and the gel/rTIMP-3 injection volume (100 μl), the estimated daily steady-state concentration level of rTIMP-3 within the targeted region was about 45 ng/ml, which exceeds the computed EC_{50} (half-maximal effective concentration) from the MMP activity curve (Fig. 1A) by about twofold. With these nine injection sites as independent measurements and with experiments

repeated in triplicate, the coefficient of variation (CV) for site-site injection was 22.5%, as measured by an rTIMP-3 ELISA.

Study design and MI model

MI induction was performed in pigs (n = 50), which were then randomly assigned to one of three targeted injection groups: saline injection only (MI/saline, n = 16), hydrogel only (MI/gel, n = 17), or hydrogel/rTIMP-3 (MI/gel/rTIMP-3, n = 17). These groups were further subdivided into three protocols (Fig. 2). In the first group, LV geometry and function were assessed by echocardiography (2, 12), infarct expansion by radiopaque markers/fluoroscopy (2), and MMP interstitial activity by fluorescence and microdialysis (3). In the second group, LV and MI geometry were assessed by cMRI, and infarct size by histochemistry (12, 15). In the third group, serial LV function was assessed by echocardiography, systemic inflammation by complement-reactive protein (CRP), myocardial polymerase chain reaction (PCR) array for relative expression for determinants of ECM remodeling and inflammation, smooth muscle actin (SMA), and overall fibrillar collagen content by histomorphometry. An additional group of age-matched pigs (n = 14) served as sham controls.

Plasma troponin I concentrations were assessed 24 hours after MI induction, whereby a uniform increase in plasma troponin levels was observed across all pigs randomized to the treatment groups (Fig. 2), which fell to negligible/nondetectable levels at 3 days after MI. These results indicated that the initial myocardial injury induced by coronary ligation was equivalent in all of the pigs randomized to the different MI treatment groups.

Local rTIMP-3 release attenuates LV remodeling and infarct expansion

Representative transthoracic echocardiographic images of the LV and indices of LV geometry and function at 14 days after MI are shown in Fig. 3A. LV dilation occurred in the MI/saline and MI/gel groups compared to sham control, as identified by increased end-diastolic dimension (LVEDd) (Fig. 3B). However, LVEDd was significantly lower in the MI/gel/rTIMP-3 group compared to the saline group (Fig. 3B). LV ejection fraction (LVEF) was reduced in all MI groups, but was higher in the MI/gel/rTIMP-3 animals compared to the MI/saline animals (Fig. 3B). LV regional wall stress increased in all MI groups when compared to referent controls, but was reduced in both the MI/gel and the MI/gel/rTIMP-3 groups, indicating that the hydrogel itself and the hydrogel containing rTIMP-3 affected this biophysical parameter. Regional infarct expansion, as measured by fluoroscopic imaging of myocardial markers, increased in the MI/saline and MI/gel groups at 14 days after MI, but was significantly attenuated in animals treated with the hydrogel/rTIMP-3 (Fig. 3B). Myocardial interstitial MMP activity was higher in the MI/saline and the MI/gel groups and was significantly reduced in the MI/gel/rTIMP-3 group, similar to the levels of the sham control animals (Fig. 3B).

In light of these findings, an additional cohort of pigs (n = 3) was also subjected to MI and administered the hydrogel/rTIMP-3 injections, but before injection, the rTIMP-3 was boiled for 2 hours to remove any MMP inhibitory effects. With increasing concentrations of the denatured rTIMP-3 (10 to 100 ng/ml), relative MMP activity remained at values identical to those obtained in the absence of rTIMP-3. At 14 days after MI, the degree of LV dilation

and reduction in LVEF was not significantly different from MI/saline or MI/gel values (fig. S1). Moreover, interstitial MMP activity was the same as values obtained for the MI/saline or MI/gel groups (fig. S1). Thus, denatured rTIMP-3 had no beneficial effects on LV geometry or in vivo MMP activity after MI.

Local rTIMP-3 release improves LV geometry and reduces infarct size

Representative cMRI images of the LV short axis were taken at the level of the central point of the targeted MI region (Fig. 3C). Posterior wall thickness at the central point of the MI region was reduced in the MI/saline group, consistent with wall thinning and infarct expansion (15) (Fig. 3C), but was partially increased by hydrogel only and hydrogel/ rTIMP-3 treatments. LV end-diastolic volume (LVEDV) increased in the MI/saline and MI/ hydrogel groups compared to sham controls (Fig. 3C). This increase was prevented in the MI/hydrogel/ rTIMP-3 group, with volumes not significantly different from sham controls.

At 14 days after MI, a clearly defined MI region was visualized with TTC staining (Fig. 3D). The LV dilation and wall thinning were evident in the MI/saline sections, which were attenuated by treatment with the hydrogel/rTIMP-3, resulting in a ~50% reduction in computed MI size compared with saline-only injections.

Time course of LV remodeling after MI is modified by local rTIMP-3 release

Changes in LVEF and volumes were time-dependent (Fig. 4). LVEF was higher in the MI/gel/rTIMP-3 group 1 day after MI and remained increased for the 14-day study period compared to the other MI groups. LVEDVs were initially higher in the MI/gel and MI/gel/ rTIMP-3 groups at 1 day after MI, but animals treated with the hydrogel/rTIMP-3 did not progress to the same extent over time as the MI/saline and MI/gel groups (Fig. 4). By day 14 after MI, LV volumes were lower in the MI/gel/rTIMP-3 animals compared to MI/saline and MI/gel animals.

In addition to these measurements, tissue Doppler was used to compute an estimate of pulmonary capillary wedge pressure (PCWP)—a clinical index of increased filling pressures and progression to heart failure (16, 17). PCWP increased over time after MI for all groups, but was lower in the MI/gel/rTIMP-3 group by day 14 after MI. Surface electrocardiogram (ECG) measurements revealed that all of the pigs remained in sinus rhythm at 1 to 14 days after MI, with no arrhythmias noted in the MI/gel or MI/gel/rTIMP-3 groups during the monitoring interval. In addition, CRP levels increased in all groups immediately after MI and fell to within normal limits at later post-MI time points (Fig. 4). However, significantly lower CRP levels were observed in the early post-MI time points for the MI/gel and MI/gel/ rTIMP-3 groups, indicating that the gel injection procedure and the gel-mediated release of rTIMP-3 did not induce a generalized inflammatory response.

Local rTIMP-3 release increases myocardial TIMP-3 content and reduces MMP activity

rTIMP-3 was identified within LV myocardial extracts from the MI region at 14 days after MI for the MI/gel/rTIMP-3 group only (Fig. 5A). Immunoreactive TIMP-3 signals were visualized in remote regions, but were more intense within the MI region in the MI/gel/ rTIMP-3 group (Fig. 5, B and C). To buttress the in vivo MMP interstitial activity

measurements, we subjected LV myocardial extracts to ex vivo MMP fluorescent activity assays. MMP activity in LV myocardial extracts was higher in all MI groups compared to sham controls (Fig. 5D). However, as in the in vivo assay, MMP activity was significantly reduced in the MI/gel/ rTIMP-3 group. Membrane type 1 (MT1) MMP proteolytic activity in LV myocardial extracts taken from the MI region from pigs has been shown previously to increase from referent control myocardial values (18). In our study, LV myocardial MT1-MMP activity was unaffected in the MI/gel group, but reduced in the MI/gel/rTIMP-3 group compared with MI/saline (Fig. 5D).

Local rTIMP-3 release modifies ECM and cytokine mRNA profiles

The effects of targeted hydrogel/rTIMP-3 injections on factors involved in ECM remodeling and inflammation after MI were next examined (Fig. 6 and table S1). The amount of *MMP-9* and *TIMP-1* mRNA was reduced to near-control levels in the MI/gel/ rTIMP-3 group, whereas *TIMP-3* mRNA levels increased. These results suggest that sustained local release of rTIMP-3 altered the relative balance between *MMP* and *TIMP* mRNA levels after MI. *Interleukin-8* (*IL-8*) and the macrophage marker *CD44 antigen–like* were lower in the MI/gel/ rTIMP-3 group compared to MI/saline or MI/hydrogel groups. The mRNA levels for markers of macrophage maturation and infiltration, *monocyte chemoattractant protein-1* (*MCP-1*), and *macrophage inflammatory protein-1α* (*MIP-1α*) increased in all post-MI groups compared with sham controls, but were markedly lower in the MI/gel/rTIMP-3 group than in the other treatment groups. Thus, mRNA levels indicative of both acute and chronic inflammation were reduced with sustained rTIMP-3 release after MI.

Local rTIMP-3 release changes collagen content and myofibroblast density

Histological examination of LV sections taken from the MI region revealed myofibrillar loss and an influx of inflammatory cells in all groups (Fig. 7A). Remnant gel was observed within the MI/gel and MI/ gel/rTIMP-3 groups at 14 days after MI/injection. LV mid-myocardial sections devoid of large blood vessels were examined with respect to immunolocalization for SMA. In the referent control and remote regions, SMA staining predominated within the vasculature, whereas the predominant SMA staining within the MI region was that of interstitial cells (Fig. 7A), consistent with myofibroblasts. This myofibroblast-positive staining was increased in the MI/gel group and the MI/gel/rTIMP-3 group compared to the MI/saline group (Fig. 7B). Collagen content increased in all MI groups when compared to sham controls (Fig. 7C). However, collagen content was greatest in animals treated with hydrogel/rTIMP-3. Because there was no change in mRNA fibrillar collagen expression in the MI/gel/TIMP-3 group from MI/saline values, then this increased total collagen content is likely due to stabilization of the ECM and reduced collagen turnover.

DISCUSSION

LV remodeling after an MI can significantly contribute to the progression to heart failure (17), and as a consequence, this process remains an important therapeutic target. Both basic and clinical studies have established that an imbalance between MMP induction and TIMPs likely contributes to this process (1, 2, 4, 7, 9). Although genetic constructs and systemic

pharmacological approaches have provided a cause-effect relationship between MMP activity and post-MI remodeling (1, 2, 9, 18, 19), translation of these observations into a clinically relevant, therapeutic strategy remains to be established. Accordingly, we used a large animal model and targeted TIMP augmentation through regional injection of a gel containing rTIMP-3 (gel/rTIMP-3) to define the effects and mechanisms on the post-MI remodeling process.

Our gel released rTIMP-3 within the MI region, controlled by both the ester-mediated hydrolysis of the gel and binding between rTIMP-3 and the HA backbone. Through this delivery approach coupled with multimodal imaging and in vivo/ex vivo measures of ECM structure/function, the new and unique findings from the present study were threefold. First, regional gel/rTIMP-3 injections abrogated infarct expansion, reduced LV dilation and regional wall stress, and improved systolic function in the early post-MI period. Second, local gel/rTIMP-3 delivery augmented total TIMP-3 levels within the MI region and reduced myocardial interstitial MMP activity without causing significant collagen accumulation over and above that of gel delivery alone. Third, rTIMP-3 release within the MI region reduced local proinflammatory cytokine levels and increased an index of myofibroblast density. We provide here proof of concept that regional, sustained delivery of an rTIMP effectively interrupts infarct expansion and improves LV geometry in a large animal heart, likely through modifying biological mediators of the adverse post-MI remodeling process.

Although the initial myocardial injury was equivalent across groups (similar troponin levels), hence addressing an important confounding variable, the natural history of post-MI remodeling diverged significantly with gel/rTIMP-3 injections. Second, the potential effects of gel injection alone on post-MI remodeling were considered. Specifically, hydrogels, as well as other biomaterials, in and of themselves can alter the mechanical/biological properties of the MI region (11, 12). We built on these observations by designing degradable hydrogels that released a recombinant protein that could directly interfere with the enzymes responsible for adverse post-MI remodeling. Specifically, the gel/rTIMP-3 injections improved LV pump function, reduced chamber dilation, and abrogated MI expansion—all effects not observed with the hydrogel injections alone. These findings hold translational importance in that the use of hydrogels in the context of post-MI remodeling can be exploited not only for intrinsic biophysical effects of the gel itself but also as a platform for localized release and targeting of specific pathways contributory to the adverse remodeling process.

In addition to reducing LV dilation, gel/rTIMP-3 injections resulted in an increase in LVEF —a key measure of global pump function. LVEF, as with any index of LV pump function, is influenced by loading conditions such as circumferential wall stress, which was reduced with gel/rTIMP-3 injections. Thus, one likely mechanism for the improved LVEF with rTIMP-3 injection was favorable effects on regional LV afterload. In addition, the reduction in LV peak circumferential stress with gel/rTIMP-3 injections would likely reduce the mechanical stress within the MI region, which would, in turn, reduce a potential stimulus for infarct expansion. Through serial studies, the changes in LVEF were attenuated early and were sustained throughout the post-MI observation period in animals treated with the hydrogel/ rTIMP-3. Therefore, this treatment approach may limit the invariable decline in

LV pump function, which occurs after MI. In these serial studies, initial LV dilation in the early post-MI time point (24 hours) appeared greater with hydrogel injections, which may be due to initial effects of polymerization and localized changes in myocardial geometry. Although this remains speculative, these serial measurements clearly demonstrate that the attenuation in LV dilation over time in the gel/rTIMP-3 group was not simply due to lower LV volumes in the initial post-MI period. A fundamental physiological variable responsible for symptoms because of progressive heart failure after MI is PCWP (16, 17). With targeted gel/rTIMP-3 injections, this physiological index of heart failure progression was attenuated, suggesting that this treatment approach altered the natural history not only of the post-MI remodeling but also of the heart failure process itself.

Targeted gel/rTIMP-3 injections reduced direct and ex vivo measures of MMP activity within the MI region, demonstrating a localized MMP inhibitory effect of rTIMP-3. Furthermore, this treatment approach reduced *MMP-9* mRNA levels. Past transgenic animal studies have identified that MMP-9 can directly contribute to adverse MI remodeling (19), and thus, reduction in MMP-9 expression with rTIMP-3 injections would yield a favorable effect on this process. However, multiple substrates and biological pathways are influenced by MMPs, and therefore, it would be an oversimplification to assume that rTIMP-3 delivery merely inhibited matrix proteolysis. For example, with gel/TIMP-3 injections, a reduction in TIMP-1 also occurred, leaving the basis for the reduction yet unclear. Nevertheless, clinical studies have suggested that increased TIMP-1 levels can be associated with adverse outcomes in the context of heart failure (1, 16). In addition, it has been demonstrated that TIMP-3 can induce direct biological effects including fibroblast function and cytokine processing (8, 9, 20, 21). We did notice shifts in expression of inflammatory markers and immune cell expression that suggested lower macrophage accumulation and polarization with hydrogel/rTIMP-3 injections, and thereby altered key aspects in chronic inflammation and impaired wound healing. It is likely that the reduction in MI wall thinning and infarct expansion with rTIMP-3 delivery was a summation of all of these biological effects.

rTIMP-3 delivery caused a shift in fibroblast phenotype as evidenced by increased SMA staining, consistent with increased myofibroblast density (22, 23). Because myofibroblasts are critical in the wound-healing context and provide significant contractile force across the matrix (1, 23), it is likely that the increase in this fibroblast phenotype with rTIMP-3 delivery influenced regional tissue geometry and structure within the MI region. Although the hydrogel-mediated release of rTIMP-3 significantly reduced MMP activity within the MI region and altered MMP/TIMP expression profiles and indices of inflammation and fibroblast transformation, these effects were not associated with a robust profibrotic response. A small and directionally similar increase in collagen content occurred in the gel only and gel/rTIMP-3 groups. These findings suggest that localized rTIMP-3 augmentation did not disproportionally alter ECM turnover and accelerate fibrosis. On the basis of the findings from the present study, future studies that define whether and to what degree localized delivery of rTIMP-3 influences ECM structure and function, as well as local stiffness properties, are warranted.

There are several limitations to this study. Adult pigs were used for MI induction because this model results in uniformity of MI size and temporal changes in infarct expansion and

LV geometry (2, 12, 14). Future studies carried out over longer observation periods with respect to the effects of localized rTIMP-3 release on post-MI remodeling and heart failure progression are warranted. On the basis of the proof-of-principle studies described here, future dose-titration studies will be required to determine the minimal threshold levels of rTIMP-3 release to significantly affect LV regional geometry and function after MI. Furthermore, although the present study provided unique mechanistic insight regarding the likely biological importance of TIMP-3 in the post-MI remodeling process, it remains to be established whether and to what degree other TIMP constructs would impart similar effects in terms of impeding infarct expansion.

Adult pigs display similar coronary anatomy, response to ischemia, and a natural history of infarct expansion to that of humans (14). Thus, the measurements of LV function and geometry used in the present study can be considered in a clinical context. We used a gel/rTIMP-3 formulation that would be immediately relevant in the context of cardiac surgery, where targeting of the MI would be feasible through direct visualization and intramyocardial injections. The concept of direct myocardial injection of biomaterials, such as alginates, has been advanced to clinical trials (24). An optimal surgical window for coronary revascularization and exposure of the MI exists within about 5 to 7 days and would allow for localized injections (25), such as those performed in our study. In sum, we describe a new therapeutic paradigm that modulates the biology of MI and the infarct expansion process by acting locally on matrix proteolytic pathways. By using materials and surgical processes similar to those used in patients, translation of this paradigm is a clinical possibility.

MATERIALS AND METHODS

Study design

Rationale and study design—The approach here was to inject a degradable HA hydrogel containing rTIMP-3 in a specific location in the heart of a large animal model of MI. The study endpoints were the effects of this treatment strategy on key indices of LV remodeling as measured by multimodality imaging (echocardiography, fluoroscopy, and MRI). Power calculations were initially performed with echocardiography-based LVEDd as the primary response variable, whereby a 20% reduction in this variable from MI-only values in the MI/gel/rTIMP-3 group, using a P value of 0.05 and β value of 0.15, would yield statistical power of 85% with a minimum sample size of 4 in each treatment group (nQuery Advisor, Statistical Solutions).

Randomization and blinding—The treatment assignments were predetermined, and each animal was assigned a code number, which was not broken until the completion of the full protocol. Thus, the LV function, biochemical, and histological measurements described herein were performed in a blinded fashion.

Replication—Sample sizes for each protocol and experimental measurement are provided in the figure legend or text, as appropriate.

rTIMP-3 and hydrogel synthesis

Human rTIMP-3 and poly-His–tagged rTIMP-3 were produced in Chinese hamster ovary cells as detailed in Supplementary Methods. The rTIMP-3 product was validated in terms of inhibitory properties with an MMP fluorescent assay as described previously (3) and further detailed in Supplementary Methods. A degradable hydrogel was fabricated by synthesizing HA macromers. HA (74 kD, Lifecore) was chemically modified with a hydroxyethyl methacrylate (HEMA) group to incorporate reactivity for hydrogel crosslinking as well as hydrolytic degradation. The full synthesis protocol is provided in Supplementary Methods. Briefly, HEMA was reacted with succinic anhydride via a ring opening polymerization in the presence of *N*-methylimidazole to obtain HEMA-COOH, which was then coupled to a tetrabutylammonium salt of HA in the presence of 4-dimethylaminopyridine. The resulting HA macromer with HEMA group modification (HEMA-HA) was purified with dialysis and characterized by ^{1}H nuclear magnetic resonance to have a modification of ~15%. The rTIMP-3 (0.20 μg/μl) was mixed with a 4 weight percent (wt %) HEMA-HA macromer solution in PBS, and the hydrogels were formed upon mixing 10 mM ammonium persulfate/tetramethylethylene diamine (APS/TEMED) initiators.

Hydrogel injection

Yorkshire pigs (n = 7, 25 kg, Hambone Farms) were anesthetized with isoflurane (2%), and through a left thoracotomy, the LV free wall was exposed. All animals were treated and cared for in accordance with the National Institutes of Health *Guide for the Care and Use of Laboratory Animals* (26), and all protocols were approved by the University of South Carolina's Institutional Animal Care and Use Committee. A square calibrated grid was sutured below the origin of the first two obtuse marginal arteries of the circumflex artery (OM1 and OM2) (2, 12), which provided for a total of nine distinct injection sites within a targeted 2 × 2–cm^2 region of myocardium. The myocardial injection strategy for the HA gel containing rTIMP-3 was an open surgical method, whereby this injection approach has been used in large animal models and in human subjects previously (11, 12, 24). In the first HA gel validation study, the hydrogel precursor and rTIMP-3 solution [100 μl; 4 wt % HEMA-HA, 10 mM APS/TEMED, rTIMP-3 (0.20 μg/μl)] were injected directly into the mid-myocardium of each target site as shown in Fig. 1E. The perimeter of the injection grid was marked at each corner with radiopaque markers, and successful injection was visualized as described in Supplementary Methods. LV samples were collected from the injection site at 7 days after injection (n = 3) and subjected to His ELISA for rTIMP-3 as detailed in Supplementary Methods. Additional histological studies were performed at 24 and 48 hours after injection and subjected to histological examination for the purposes of HA gel localization. In the final validation study (n = 3), myocardial, liver, kidney, and lung samples as well as plasma were collected at 7 days after injection and subjected to human rTIMP-3 immunoassay (Supplementary Methods). This injection strategy for HA gel deliver with and without rTIMP-3 was then carried forward to the MI protocols.

MI porcine model

Pigs were anesthetized, and markers were placed as described in the 2 × 2 grid. OM1 and OM2 were ligated to induce an MI, and characteristic ECG changes occurred, but electrical

cardioversion and/or defibrillation were not required. After MI induction, nine injections were performed with the precalibrated grid, where the injections were saline, gel, or gel/rTIMP-3. Three different protocols were executed to examine the effects of gel/rTIMP-3 injections upon key determinants of the post-MI remodeling process (Fig. 2), described below and in more detail in Supplementary Methods.

Protocol 1: LV geometry, infarct expansion, and in vivo MMP activity—At 14 days after MI or control procedures, echocardiography was performed to calculate LV dimensions and ejection fraction (2, 12). Fluoroscopic images of the myocardial markers were recorded with high-speed cinefluoroscopy (2, 12). After imaging studies, the pigs were anesthetized, the LV was exposed through a sternotomy, and a microdialysis probe (outside diameter of probe shaft, 0.77 mm; CMA Microdialysis) was placed within the MI region and infused with an MMP fluorescent substrate (Enzo) (3). The fluorescent signal was normalized to sham control referent values to compare differences between treatment groups.

Protocol 2: cMRI and ex vivo measurements of infarct size—Fourteen days after MI or control procedures, cMRI was performed with retrospectively gated 3D steady-state free precession cine MRI for volumetric analysis (15). Fifteen minutes after intravenous injection of gadobenate dimeglumine (0.1 mmol/kg), infarct location and wall thickness were visualized with a 3D late gadolinium–enhanced approach. After cMRI measurements, the LV was harvested and subjected to histochemical staining and direct infarct size quantitation with TTC.

Protocol 3: Serial measurements of LV function and geometry—For these studies, pigs were instrumented as described in the preceding section with the addition of a vascular access catheter placed in the descending aorta. LV echocardiography and blood samples (5 ml) were collected at baseline and then at 1, 2, 7, and 14 days after MI. The collected blood samples were centrifuged, and the decanted plasma was subjected to ELISA for troponin I (KT-474, Kamiya Biomedical Co.) and CRP (IPGCRPKT, Innovative Research Inc.). Surface ECG recordings were also collected at each time point.

Immunoassays, MMP activity, PCR, and histochemistry

Immunoblotting was performed for total myocardial TIMP-3 using approaches described in detail previously and in Supplementary Methods (2, 7, 12). In addition, rTIMP-3 measurements were performed by ELISA, whereby the intra-assay CV was 8.7%. LV myocardial extracts (50 μg) were incubated with the global MMP substrate as well as with an MT1-MMP–specific fluorescent substrate (Enzo and Calbiochem, respectively, both 60 μM, for 2 hours at 37°C) (23). RNA was extracted from LV samples (RNeasy, Qiagen), and reverse transcription PCR was performed with gene/pig-specific primer/probe sets (table S2) and described in further detail in Supplementary Methods. The formalin-fixed LV samples were sectioned and stained with picrosirius red for fibrillar collagen or for SMA and then subjected to morphometric measurements. Additional LV sections were stained with H&E, and histopathological examination was performed.

Statistical analysis

Statistical analyses were performed with STATA statistical software (STATA Corp.). LV geometry, function, and indices of MI area were compared between the control and MI groups with a one-way ANOVA. Post hoc separation after ANOVA was performed using pairwise comparisons with Bonferroni corrections (prcomp module, STATA). The interstitial global MMP activity was evaluated by ANOVA and subsequently compared against the control values of 100% by a Student's t test. For TIMP-3 levels and plasma troponin and CRP concentrations, values from each group were first evaluated by ANOVA, and then a post hoc separation following ANOVA was performed using pairwise comparisons with a Bonferroni analysis. A similar approach was taken for the morphometric measurements. For the PCR results, normality of the data was not assumed, and thus, comparisons were performed with nonparametric analogs of the ANOVA (Kruskal-Wallis) and pair-wise comparisons by the median test. Results are presented as means ± SEM. $P < 0.05$ was considered to be statistically significant.

Supplementary Material

Refer to Web version on PubMed Central for supplementary material.

Acknowledgments

We acknowledge the technical expertise of R. Stroud, R. K. Patel, and M. Oelsen (Medical University of South Carolina).

Funding: This work was supported by NIH grants HL057952, HL059165, and HL095608 and a Merit Award from the Veterans' Affairs Health Administration. S.R.E. and B.P.P. were supported by NIH grants T32HL007260 and T32HL007954, respectively. R.C.G., J.A.B., and F.G.S. provided funding for the studies.

Reference and notes

1. Spinale FG. Myocardial matrix remodeling and the matrix metalloproteinases. Influence on cardiac form and function. Physiol. Rev. 2007; 87:1285–1342. [PubMed: 17928585]
2. Mukherjee R, Brinsa TA, Dowdy KB, Scott AA, Baskin JM, Deschamps AM, Lowry AS, Escobar GP, Lucas DG, Yarbrough WM, Zile MR, Spinale FG. Myocardial infarct expansion and matrix metalloproteinase inhibition. Circulation. 2003; 107:618–625. [PubMed: 12566376]
3. Spinale FG, Koval CN, Deschamps AM, Stroud RE. Dynamic changes in matrix metalloproteinase activity within the human myocardial interstitium during ischemia reperfusion. Circulation. 2008; 118(Suppl. 14):S16–S23. [PubMed: 18824748]
4. Webb CS, Bonnema DD, Ahmed SH, Leonardi AH, McClure CD, Clark LL, Stroud RE, Corn WC, Finklea L, Zile MR, Spinale FG. Specific temporal profile of matrix metalloproteinase release occurs in patients following myocardial infarction: Relation to left ventricular remodeling. Circulation. 2006; 114:1020–1027. [PubMed: 16923753]
5. Dormán G, Cseh S, Hajdú I, Barna L, Kónya D, Kupai K, Kovács L, Ferdinandy P. Matrix metalloproteinase inhibitors: A critical appraisal of design principles and proposed therapeutic utility. Drugs. 2010; 70:949–964. [PubMed: 20481653]
6. Brew K, Dinakarpandian D, Nagase H. Tissue inhibitors of metalloproteinases: Evolution, structure and function. Biochim. Biophys. Acta. 2000; 1477:267–283. [PubMed: 10708863]
7. Wilson EM, Moainie SL, Baskin JM, Lowry AS, Deschamps AM, Mukherjee R, Guy TS, St John-Sutton MG, Gorman JH III, Edmunds LH Jr, Gorman RC, Spinale FG. Region and species specific induction of matrix metalloproteinases occurs with post-myocardial infarction remodeling. Circulation. 2003; 107:2857–2863. [PubMed: 12771000]

8. Lovelock JD, Baker AH, Gao F, Dong JF, Bergeron AL, McPheat W, Sivasubramanian N, Mann DL. Heterogeneous effects of tissue inhibitors of matrix metalloproteinases on cardiac fibroblasts. Am. J. Physiol. Heart Circ. Physiol. 2005; 288:H461–H468. [PubMed: 15650153]
9. Kassiri Z, Defamie V, Hariri M, Oudit GY, Anthwal S, Dawood F, Liu P, Khokha R. Simultaneous transforming growth factor β-tumor necrosis factor activation and cross-talk cause aberrant remodeling response and myocardial fibrosis in Timp3-deficient heart. J. Biol. Chem. 2009; 284:29893–29904. [PubMed: 19625257]
10. Yu WH, Yu S, Meng Q, Brew K, Woessner FJ Jr. TIMP-3 binds to sulfated glycosaminoglycans of the extracellular matrix. J. Biol. Chem. 2000; 275:31226–31232. [PubMed: 10900194]
11. Ifkovits JL, Tous E, Minakawa M, Morita M, Robb JD, Koomalsingh KJ, Gorman JH III, Gorman RC, Burdick JA. Injectable hydrogel properties influence infarct expansion and extent of postinfarction left ventricular remodeling in an ovine model. Proc. Natl. Acad. Sci. U.S.A. 2010; 107:11507–11512. [PubMed: 20534527]
12. Mukherjee R, Zavadzkas JA, Saunders SM, McLean JE, Jeffords LB, Stroud RE, Leone AM, Koval CN, Rivers WT, Basu S, Sheehy A, Michal G, Spinale FG. Targeted myocardial micro-injections of a biocomposite material reduces infarct expansion in pigs. Ann. Thorac. Surg. 2008; 86:1268–1276. [PubMed: 18805174]
13. Lee RJ, Hinson A, Helgerson S, Bauernschmitt R, Sabbah HN. Polymer-based restoration of left ventricular mechanics. Cell Transplant. 2013; 22:529–533. [PubMed: 22469060]
14. Dixon JA, Spinale FG. Large animal models of heart failure: A critical link in the translation of basic science to clinical practice. Circ. Heart Fail. 2009; 2:262–271. [PubMed: 19808348]
15. Blom AS, Pilla JJ, Arkles J, Dougherty L, Ryan LP, Gorman JH III, Acker MA, Gorman RC. Ventricular restraint prevents infarct expansion and improves borderzone function after myocardial infarction: A study using magnetic resonance imaging, three-dimensional surface modeling, and myocardial tagging. Ann. Thorac. Surg. 2007; 84:2004–2010. [PubMed: 18036925]
16. Zile MR, Desantis SM, Baicu CF, Stroud RE, Thompson SB, McClure CD, Mehurg SM, Spinale FG. Plasma biomarkers that reflect determinants of matrix composition identify the presence of left ventricular hypertrophy and diastolic heart failure. Circ. Heart Fail. 2011; 4:246–256. [PubMed: 21350055]
17. Colucci, WS.; Braunwald, E. Braunwald's Heart Disease: A Textbook of Cardiovascular Medicine. Philadelphia, PA: Elsevier; 2005. Pathophysiology of Heart Failure.
18. Spinale FG, Janicki JS, Zile MR. Membrane-associated matrix proteolysis and heart failure. Circ. Res. 2013; 112:195–208. [PubMed: 23287455]
19. Ducharme A, Frantz S, Aikawa M, Rabkin E, Lindsey M, Rohde LE, Schoen FJ, Kelly RA, Werb Z, Libby P, Lee RT. Targeted deletion of matrix metalloproteinase-9 attenuates left ventricular enlargement and collagen accumulation after experimental myocardial infarction. J. Clin. Invest. 2000; 106:55–62. [PubMed: 10880048]
20. Amour A, Slocombe PM, Webster A, Butler M, Knight CG, Smith BJ, Stephens PE, Shelley C, Hutton M, Knäuper V, Docherty AJ, Murphy G. TNF-α converting enzyme (TACE) is inhibited by TIMP-3. FEBS Lett. 1998; 435:39–44. [PubMed: 9755855]
21. Leco KJ, Khokha R, Pavloff N, Hawkes SP, Edwards DR. Tissue inhibitor of metalloproteinases-3 (TIMP-3) is an extracellular matrix-associated protein with a distinctive pattern of expression in mouse cells and tissues. J. Biol. Chem. 1994; 269:9352–9360. [PubMed: 8132674]
22. Frangogiannis NG. Regulation of the inflammatory response in cardiac repair. Circ. Res. 2012; 110:159–173. [PubMed: 22223212]
23. Baum J, Duffy HS. Fibroblasts and myofibroblasts: What are we talking about? J. Cardiovasc. Pharmacol. 2011; 57:376–379. [PubMed: 21297493]
24. LoneStar Heart Inc. A randomized, controlled study to evaluate Algisyl-LVR™ as a method of left ventricular augmentation for heart failure (AUGMENT-HF). 2011–2012. NLM identifier: NCT01311791; http://clinicaltrials.gov/ct2/show/NCT01311791
25. Lee DC, Oz MC, Weinberg AD, Ting W. Appropriate timing of surgical intervention after transmural acute myocardial infarction. J. Thorac. Cardiovasc. Surg. 2003; 125:115–119. [PubMed: 12538993]
26. NIH. Guide for the Care and Use of Laboratory Animals. Washington, DC: NIH; 2011. p. 8

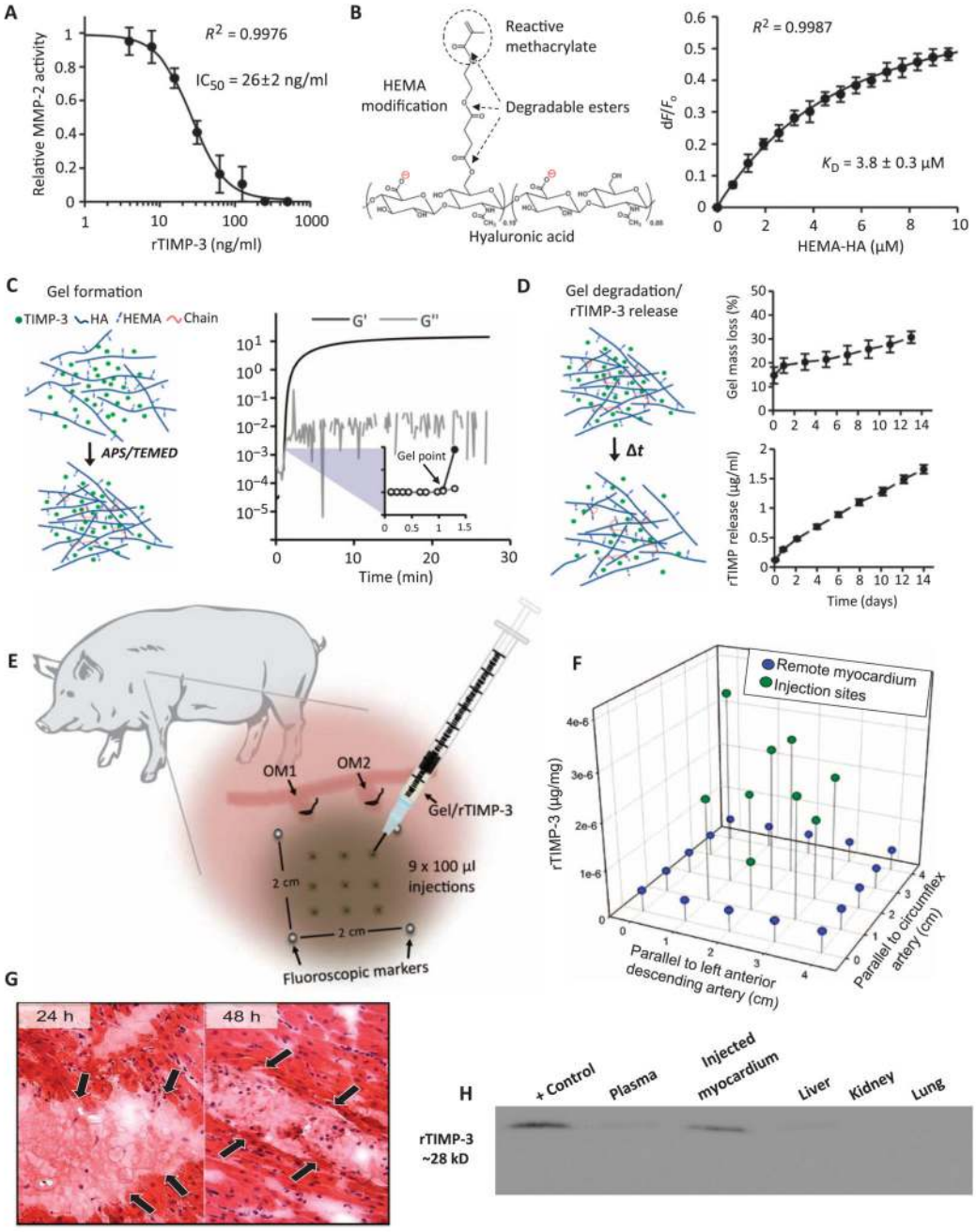

Fig. 1. rTIMP-3 validation and hydrogel fabrication for targeted rTIMP-3 delivery

(**A**) rTIMP-3 inhibition of MMP-2 and computed inhibitory concentration (IC_{50}). Data are means ± SEM (n = 3) and are fit to a four-parameter logistic equation. (**B**) HA macromer with reactive methacrylate groups for hydrogel cross-linking and hydrolytically unstable ester groups for gel degradation. The negatively charged macromer binds to rTIMP-3 through electrostatic interactions with a predicted disassociation constant (K_D, right panel). Data are means ± SEM (n = 3) and are fit to a bimolecular association equation. (**C**) Representative gel crosslinking schematic and quantification with rheometry by measuring

the storage (G′) and loss (G″) moduli after mixing initiators with HA macromers. Crosslinking reaction reached a gel point in about 1 min (inset). (**D**) Gel degradation and rTIMP-3 release quantification with a uronic acid assay and enzyme-linked immuno-sorbent assay (ELISA), respectively, over 14 days. Data are means ± SEM (n = 3). (**E**) Injection schematic (nine injections using a calibrated grid) of gels containing 20 μg of rTIMP-3 per 100-μl injection into the myocardial region targeted for MI (region served by coronary arteries OM1 and OM2). (F)rTIMP-3 quantified at the nine injections sites in (E) and remote regions 1 week after injection, plotted in a three-dimensional (3D) array. Data are means + SEM (n = 3). (**G**) Representative histological section shows HA gel localized to the mid-myocardial injection sites at 24 hours (n = 2) and 48 hours (n = 2) after injection (arrows; original magnification, ×40). (**H**) His-tagged rTIMP-3 examined by immunoblotting at 7 days after injection at the myocardial injection site, at other organs, and in the circulation.

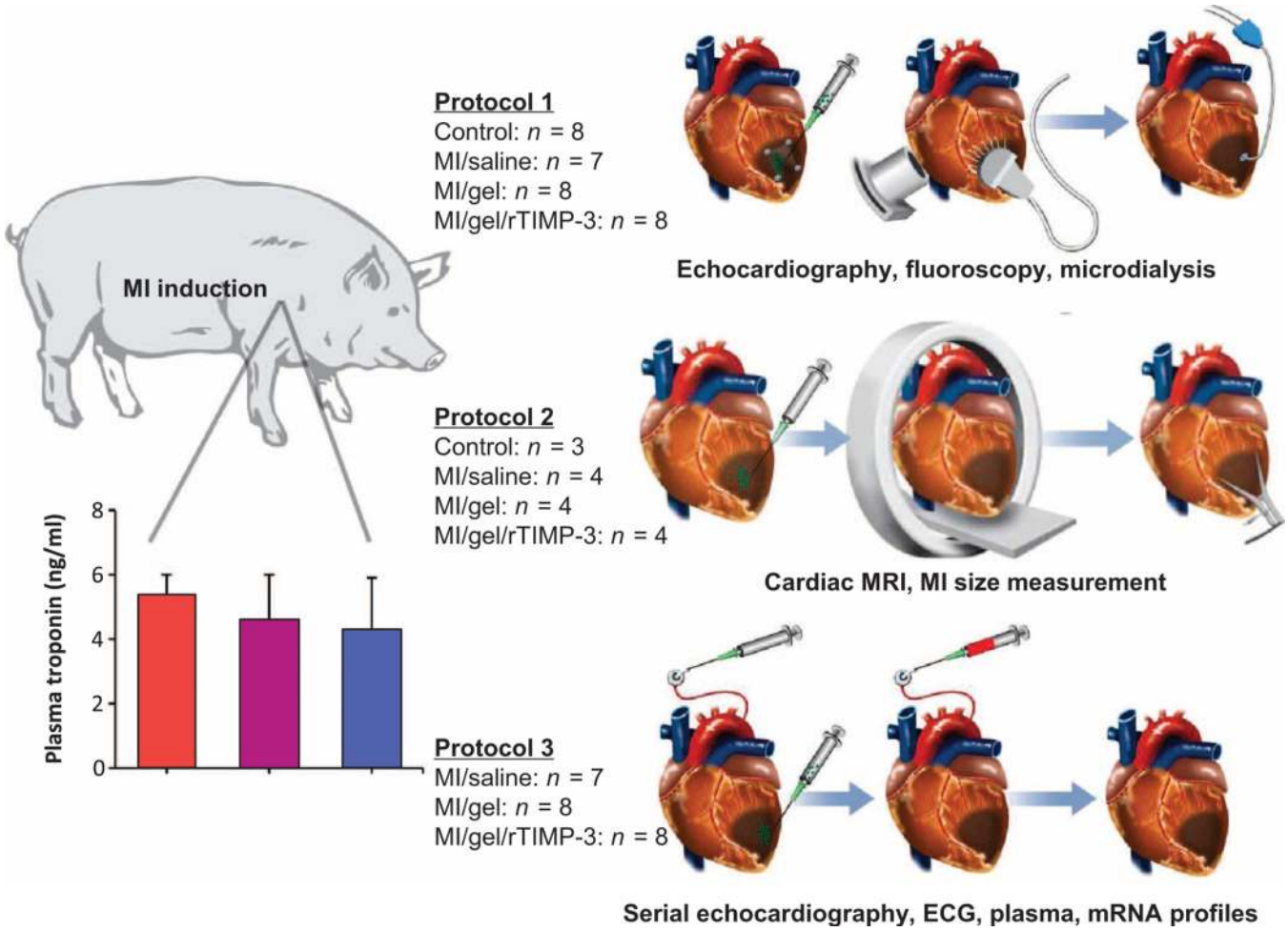

Fig. 2. Schematic of experimental design and protocol assignments

Adult pigs (n = 50) underwent MI induction by coronary ligation and were then randomized to three different treatments: MI/saline (saline injections), targeted injection of a degradable HA-based gel (MI/gel), or targeted injection of gel containing rTIMP-3 (MI/gel/rTIMP-3; 9- to 100-μl injections, 0.2 μg/μl per injection) and followed for 14 days. Instrumented pigs with no MI induction served as referent sham controls (n = 14). Plasma troponin levels drawn at 24 hours were equivalent ($P > 0.05$) across treatment group assignments (post hoc pairwise comparisons by Bonferroni corrections), indicating an equivalent degree of initial myocardial injury. Data are means + SEM. After treatment assignment, the pigs were assigned to one of three different protocols, as shown.

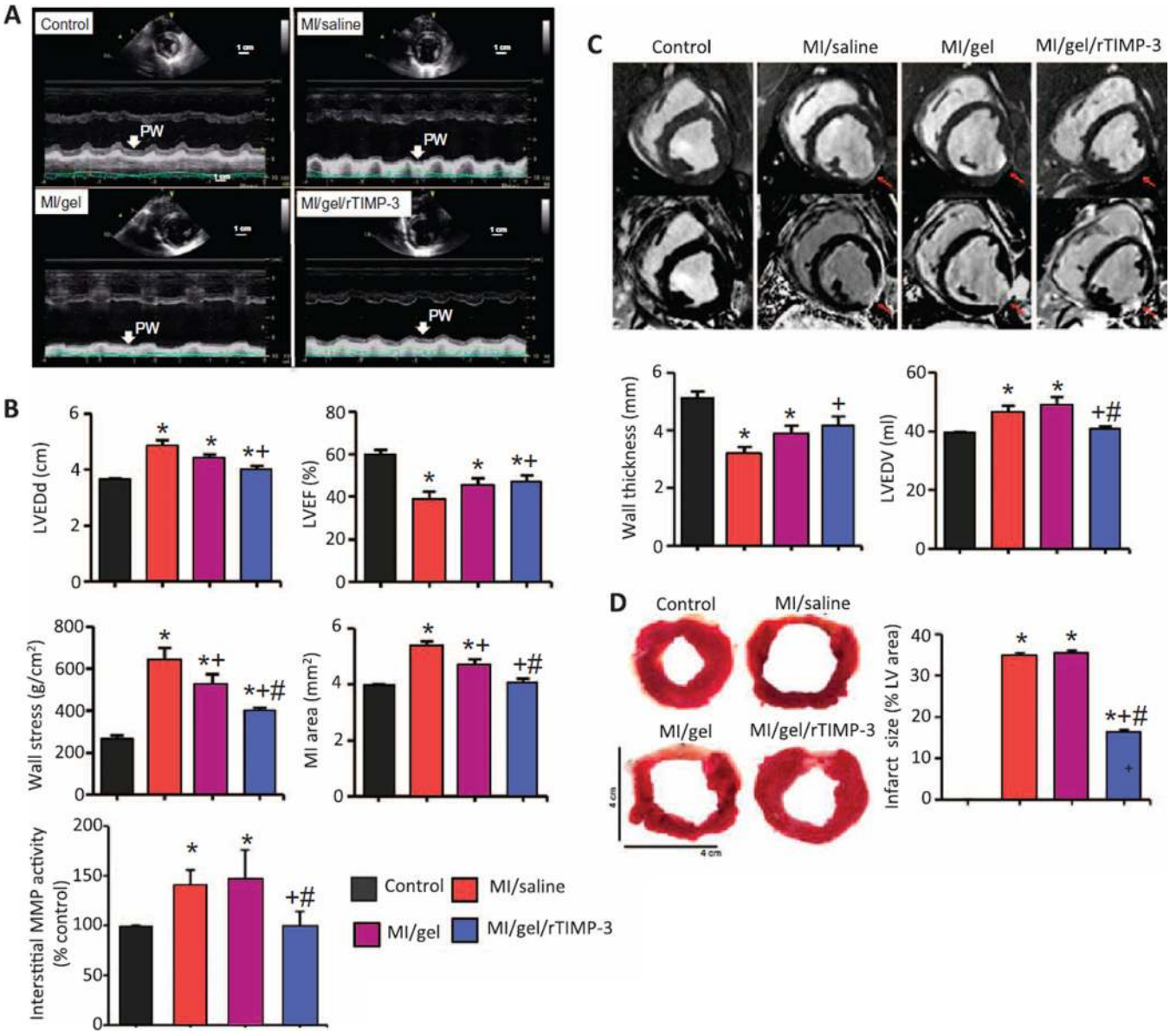

Fig. 3. LV remodeling and infarct expansion attenuated by local rTIMP-3 release

(**A**) Representative images across the LV septum and posterior wall (PW) using echocardiography in an instrumented non-MI (sham) control and all three MI treatment groups. (**B**) LVEDd, LVEF, LV peak wall stress, MI area, and MMP interstitial activity (normalized to sham control interstitial fluorescent values) within the MI region 14 days after MI. Data are means ± SEM (n = 8 controls, 7 MI/saline, 8 MI/gel, and 8 MI/gel/rTIMP-3). (**C**) cMRI was performed in referent controls (sham), MI/saline, MI/gel, and MI/gel/rTIMP-3 at 14 days after MI. Representative short-axis views at end-diastole are shown. The red arrow indicates the posterior wall at the central point of the MI. Data are means ± SEM (n = 3 controls, 4 MI/saline, 4 MI/gel, and 4 MI/gel/rTIMP-3). (**D**) Tetraphenyl tetrazolium chloride (TTC) staining at the site of the MI and quantification of infarct size. There was no infarct identified in the referent controls, and hence, the value is

zero. Data are means ± SEM (n = 3 controls, 4 MI/saline, 4 MI/gel, and 4 MI/gel/rTIMP-3). For (B) to (D), P values were determined by analysis of variance (ANOVA) followed by post hoc pairwise comparisons by Bonferroni corrections. $^{*}P < 0.05$ versus control, $^{+}P < 0.05$ versus MI/saline, $^{\#}P < 0.05$ versus MI/gel.

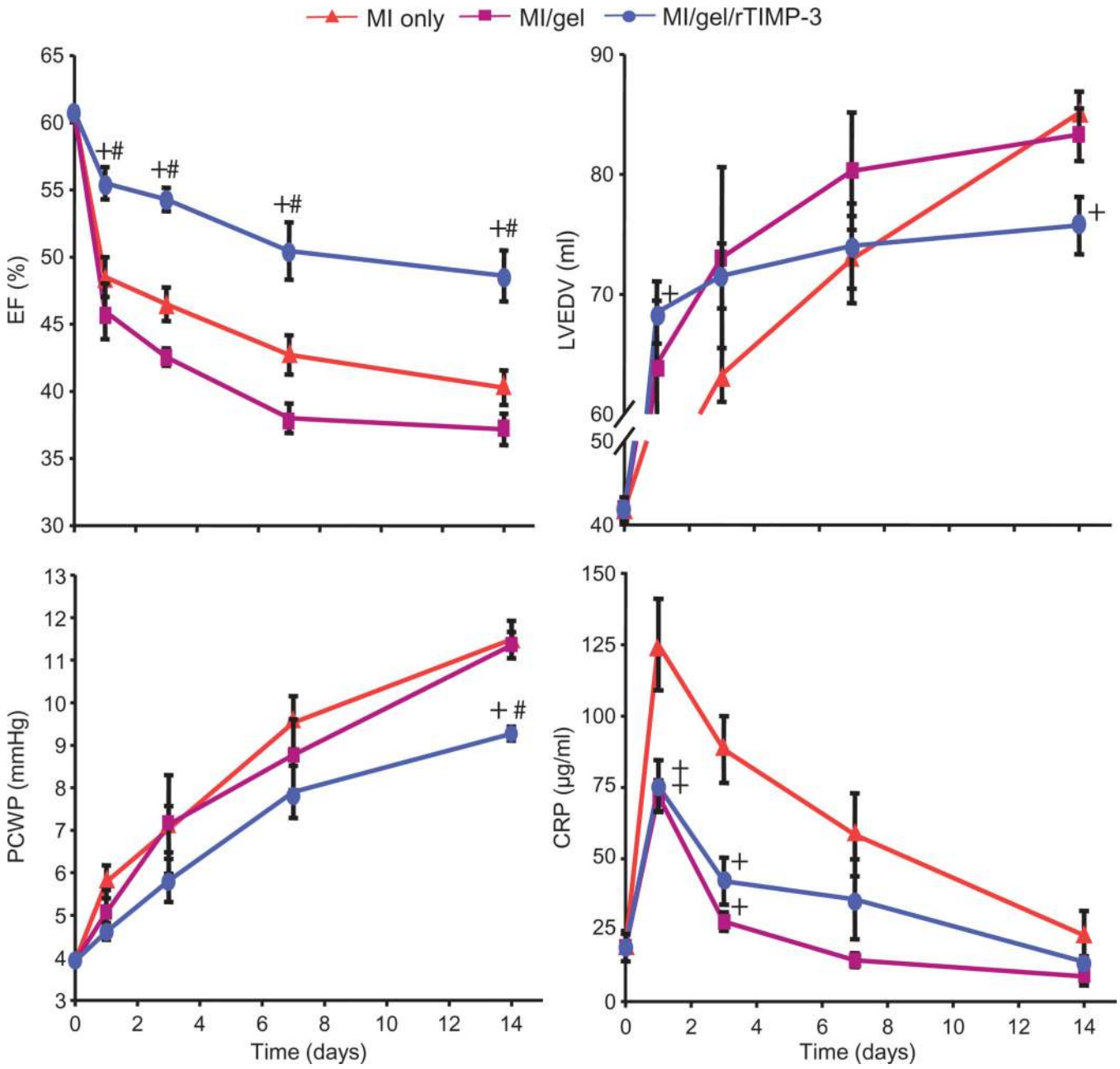

Fig. 4. Serial LV echocardiography after MI: Effects of targeted rTIMP-3 delivery

LVEF, LVEDV, PCWP, and plasma CRP were measured at baseline and at 1, 3, 7, and 14 days after MI. Data are means ± SEM ($n = 5$). In all groups, LVEF fell after MI, and LVEDV and PCWP increased compared to baseline (all $P < 0.05$; not marked on plots for clarity). For individual-day comparisons, $^{+}P < 0.05$ versus MI/saline (MI only), $^{\#}P < 0.05$ versus MI/gel, post hoc pairwise comparisons by Bonferroni corrections.

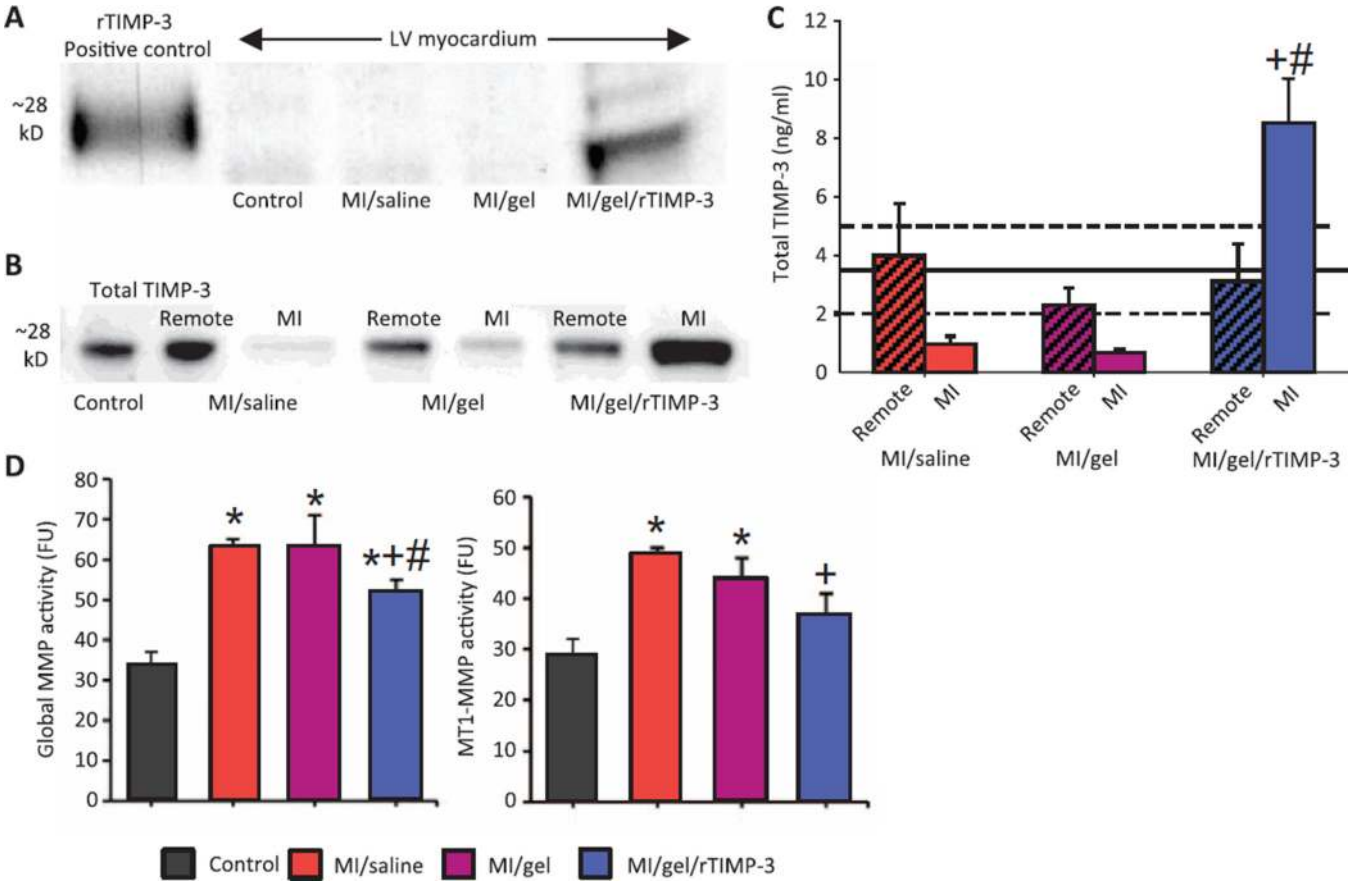

Fig. 5. Total TIMP-3 levels are augmented, and MMP activity is reduced with targeted rTIMP-3 delivery

(**A**) His-tagged rTIMP-3 was identified by immunoblot-ting. (**B**) A representative immunoblot for using antisera, which reacted against both rTIMP-3 and native TIMP-3. (**C**) Total LV myocardial TIMP-3 levels within the MI and remote regions at 14 days after MI as well as in control samples. The remote region constitutes the noninjected, nonischemic myocardial region served by coronary circulation independent of the targeted ligation sites shown in Fig. 1E. The mean is represented by the solid line, and the SEM is represented by the dashed lines ($n = 7$). (**D**) Ex vivo total MMP and MT1-MMP–specific activity. For (C) and (D), data are means + SEM ($n = 8$ control, 7 MI/saline, 8 MI/gel, and 8 MI/gel/rTIMP-3). FU, fluorescence units. P values were determined by ANOVA followed by post hoc pairwise comparisons by Bonferroni corrections. $^{*}P < 0.05$ versus control, $^{+}P < 0.05$ versus MI/saline, $^{\#}P < 0.05$ versus MI/gel.

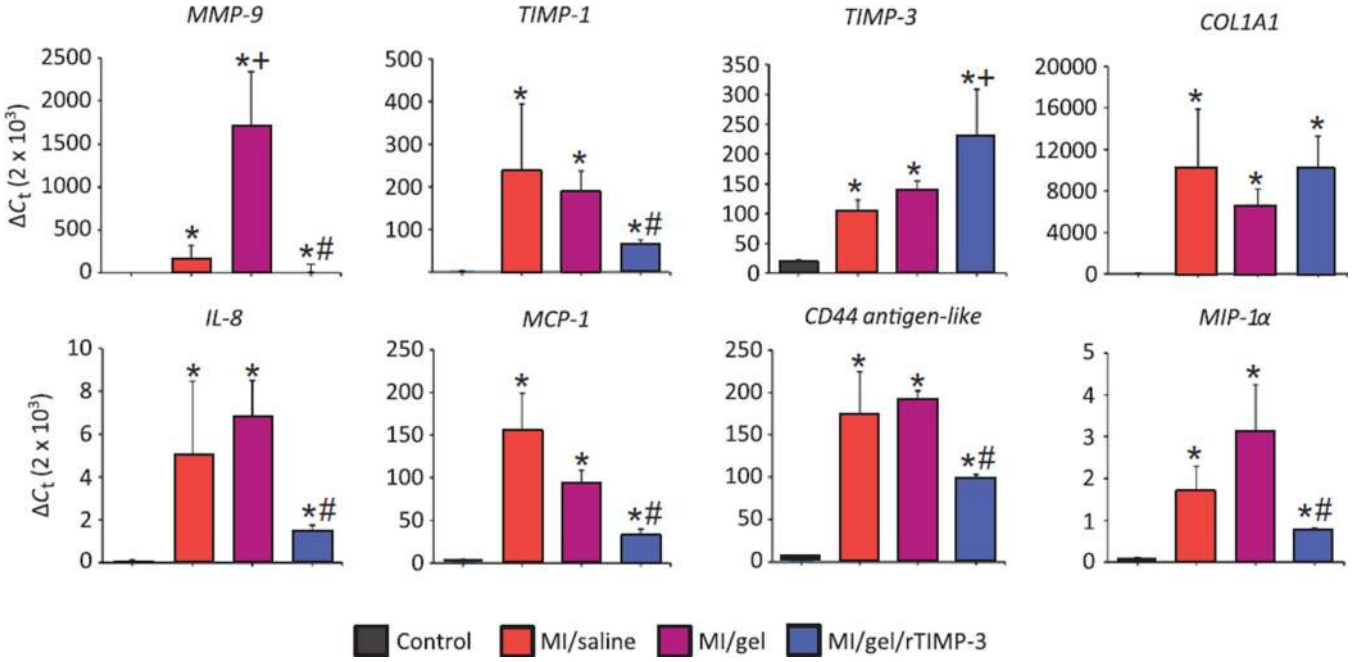

Fig. 6. Regional rTIMP-3 release alters mRNA levels for ECM and inflammatory markers after MI

Data are means + SEM (n = 8 control, 7 MI/saline, 8 MI/gel, and 8 MI/gel/rTIMP-3). P values were determined by median test. $^{*}P < 0.05$ versus control, $^{+}P < 0.05$ versus MI/saline, $^{\#}P < 0.05$ versus MI/gel.

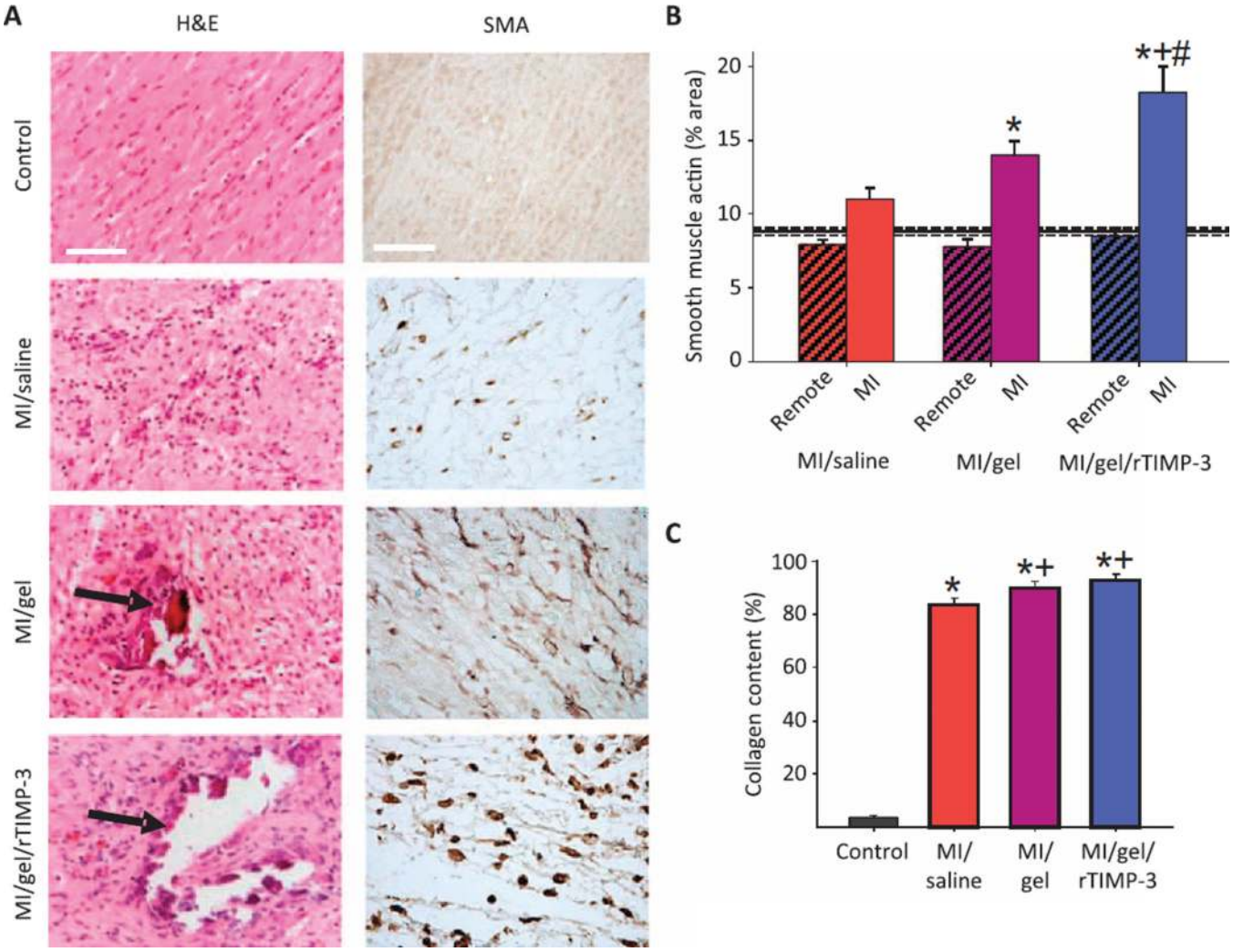

Fig. 7. Histomorphometry reveals minimal inflammation, increased fibroblast SMA content, and increased ECM content with targeted rTIMP-3 delivery

(**A**) Representative photomicrographs of LV sections taken from the MI region stained with hematoxylin and eosin (H&E) or SMA. Islands of remnant gel were observed within the MI region of the MI/gel and the MI/gel/rTIMP-3 groups (black arrows). Scale bars, 50 μm. (**B**) Quantification of SMA staining within the MI region. The referent control values are shown with mean represented as the solid line, and the SEM is represented by the dashed lines. (**C**) Morphometric measurements for fibrillar collagen. For (B) and (C), data are means + SEM (n = 3 controls, 5 MI/saline, 5 MI/gel, and 5 MI/gel/rTIMP-3). P values were determined by ANOVA followed by post hoc pairwise comparisons by Bonferroni corrections. $^{*}P < 0.05$ versus control, $^{+}P < 0.05$ versus MI/saline, $^{\#}P < 0.05$ versus MI/gel.